ZnO nanorod/multi-walled carbon nanotube nanocomposite for ethanol vapour detection

Feifei Cao[1], *Cuiping Li*[1] ✉, *Mingji Li*[1], *Hongji Li*[2], *Baohe Yang*[1]

[1]*Tianjin Key Laboratory of Film Electronic and Communicate Devices, School of Electrical and Electronic Engineering, Tianjin University of Technology, Tianjin 300384, People's Republic of China*
[2]*Tianjin Key Laboratory of Organic Solar Cells and Photochemical Conversion, School of Chemistry and Chemical Engineering, Tianjin University of Technology, Tianjin 300384, People's Republic of China*
✉ *E-mail: licp226@126.com*

Published in Micro & Nano Letters; Received on 31st October 2017; Revised on 6th February 2018; Accepted on 15th February 2018

Zinc oxide nanorods (ZnONRs) were grown directly on the generally used sensing electrodes of alumina ceramic tubes by a hydrothermal method. Multi-walled carbon nanotubes (MWCNTs) were assembled on the surface of the ZnONRs using ultrasonic dispersing. The ethanol gas sensing properties of the prepared ZnONRs sensor, MWCNTs sensor, and ZnONRs/MWCNTs nanocomposite gas sensor were investigated. The ZnONRs/MWCNTs nanocomposite sensor demonstrated a higher response, faster response-recovery, and better selectivity to ethanol than the ZnONRs and MWCNTs sensors. At an optimal working temperature of 370°C, the response to 100 ppm ethanol is 26.1 for the ZnONRs/MWCNTs nanocomposite sensor, which is much higher than those of the ZnONRs sensor (10.4) and MWCNTs sensor (5.1). A short response time of 2 s and a recovery time of 16 s are achieved for the ZnONRs/MWCNTs sensor. Moreover, the long-term stability and repeatability of the ZnONRs/MWCNTs sensor were also discussed. The improved ethanol sensing properties of the ZnONRs/MWCNTs sensor can be attributed to the synergistic effects of ZnONRs and MWCNTs, including the large specific surface area and high electron transport capability.

1. Introduction: Semiconductor metal oxides are promising materials in the field of gas sensors due to their low cost, high sensitivity, simple fabrication methods, and easily carried around [1]. Among the known semiconductor metal oxides, zinc oxide (ZnO) has attracted wide interest because of its non-toxicity, abundance in nature, controllable resistivity, and high thermal stability. However, there are still some shortcomings such as low response speed, low selectivity, high working temperature, and poor stability for ZnO gas sensors. Many techniques have been carried out to improve their gas sensing performance. Since the sensing performance is closely related to the morphology of the ZnO sensing material, various topography-controlled ZnO nanostructures with the large specific surface area have been fabricated and studied, such as nanorods, nanowires, nanoflowers, and nanobeads [2–5]. Doping with a suitable impurity, such as transition metals [6–8], noble metals (Pt, Au, and Ag), and rare earth metals [9, 10], is another widely used method to enhance the sensing behaviour of ZnO. In addition, many studies have demonstrated that ZnO composites, which consist of chemically distinct components, show more excellent sensing properties than a single ZnO [11–17]).

Carbon nanotubes (CNTs), which possess good conductivity, large specific surface areas, molecular-sized pores, and high adsorption capacities, are considered to be excellent sensing materials for a gas sensor [18, 19]. A ZnO/CNT composite structure can increase the response dramatically and lower the working temperature to certain gases [16, 17, 20]. Nanoparticles were the most used ZnO nanostructure to compose a ZnO/CNT hybrid for gas sensors [21–23]. Recently, Oweis *et al*. reported on the single-walled CNT/ZnO nanorod (ZnONR) composite for a NO_2 gas sensor with an acceptable detection range and accuracy, low cost, and light weight [17]. Farbod *et al*. prepared the ZnO hollow sphere (ZHS)/multi-walled CNT (MWCNT) composite for the detection of volatile organic compounds (VOCs) [16]. They found that the adding of CNTs to the ZHSs increased significantly the responses, decreased the optimum operating temperature, and improved the selectivity to the target VOCs.

In this work, ZnONRs were fabricated directly on the Al_2O_3 ceramic tubes using a hydrothermal process. MWCNTs were assembled on the ZnONRs surfaces to form the ZnONRs/MWCNTs nanocomposite. The gas sensing properties of the pure ZnONRs, pure MWCNTs and ZnONRs/MWCNTs nanocomposite for the detection of ethanol vapour were measured. The prepared ZnONRs/MWCNTs nanocomposite is found to exhibit a high response, short response, recovery times, good selectivity, and excellent stability.

2. Experimental details: The ZnONRs/MWCNTs nanocomposite was fabricated in two steps: (i) growth of vertically aligned ZnONRs directly onto the generally used sensing electrode of alumina ceramic tubes and (ii) formation of MWCNTs on the ZnONRs. Firstly, ZnONRs were synthesised via a hydrothermal process. Fig. 1*a* shows the diagram of the used alumina ceramic tube sensor element. Fig. 1*b* shows the photograph of the used sensor element welded on the pedestal. All the chemicals were purchased from the Tianjin Guangfu Fine Chemical Research Institute and were used as received without further purification. 0.55 g zinc acetate was dissolved in 50 ml methanol under magnetic stirring at room temperature for 2 h. The alumina ceramic tubes were immersed in the above solution for 10 min with ultrasonic vibration and then were heated at 200°C for 1 h in a muffle furnace to grow ZnO seeds. A mixed aqueous solution of 0.05 M zinc nitrate, 0.05 M hexamethylenetetramine ($C_6H_{12}N_4$), 0.05 M ammonia, and 0.002 M polyethyleneimine was transferred into Teflon-lined stainless steel autoclaves and the seeded alumina ceramic tubes were immersed in the mixed solution at 100°C for 12 h to grow the ZnONRs. The alumina ceramic tubes grown with ZnONRs were rinsed with deionised water several times. Secondly, 0.05 g MWCNT-COOH was dispersed in 10 ml ethanol by ultrasonic vibration. The MWCNTs we used were purchased from Dekedaojin in Beijing, China, which were prepared by a chemical vapour deposition method. The ceramic tubes with ZnONRs were immersed in the ultrasonic MWCNTs' suspension for 1 h and then annealed at 450°C

for 1 h in a muffle furnace to form the ZnONRs/MWCNTs nanocomposite. For comparison, the pure ZnONRs sensor and pure MWCNTs sensor were also prepared. The synthesis process of the pure MWCNTs sensor is as follows: the slurry of MWCNTs mixed with ethanol was formed and then coated onto a ceramic tube, followed by sintering the ceramic tube at 450°C for 1 h.

Surface morphologies and crystalline microstructures of the ZnONRs, MWCNTs, and ZnONRs/MWCNTs nanocomposite were characterised by field emission-scanning electron microscopy (Merlin Compact, Zeiss), high-resolution (HR) transmission electron microscopy (TEM; Philips Tecnai F20), and X-ray diffraction (XRD, Thermo Scientific, DXR) with Cu Kα radiation. The gas sensing performances were measured using a gas sensing characterisation system (WS-30A, Weisheng Electronics Co., Ltd, HeNan Province, China). The concentrations of the target gas were obtained by injecting liquid of volume Q into the testing chamber. The liquid volume Q can be calculated by the following formula [24, 25]:

$$Q = \frac{V \times \phi \times M}{22.4 \times d \times \rho} \times 10^{-9} \times \frac{273 + T_R}{273 + T_B}. \quad (1)$$

Here, V is the volume of the testing chamber, φ is the vapour concentration, M is the molecular weight of the testing gas, d and ρ are the density and purity of the liquid, respectively. T_R is the room temperature and T_B is the temperature in the testing chamber which is separated by a case from the room environment. The electronic circuit is shown in Fig. 1c. In the circuit, V_c is the circuit voltage (5 V), V_h is the heating voltage, R_L is a load resistance (47 kΩ for the ZnONRs and ZnONR/MWCNT sensors, 100 Ω for the MWCNTs sensor), V_{out} is the voltage on R_L. The response is defined as $S = R_a/R_g$, where R_a and R_g are the electrical resistance of the gas sensor in the air and in the mixture of air and testing gas, respectively. The response time and recovery time are two important parameters to evaluate the performance of the gas sensor and are defined as the time taken by the sensor to achieve 90% of the total resistance change during the gas inputting and outputting process, respectively.

3. Results and discussions: The scanning electron microscopy (SEM) images of ZnONRs, MWCNTs, and ZnONR/MWCNT nanocomposite are shown in Fig. 2. In Fig. 2*a*, uniform and homogenous ZnONRs with a diameter of ~50 nm were grown vertically on the ceramic tube. The single ZnONR exhibits a prism with a hexagonal end. Dense MWCNTs with diameters of ~50 nm twisted with each other are shown in Fig. 2*b*. Fig. 2*c* shows that MWCNTs are horizontally covered on the surfaces of the ZnONRs and intersect with the ZnONRs. We think the MWCNTs–ZnONRs attachment is formed through some physicochemical interactions such as Van der Waals force, H bonding and other bonds [26].

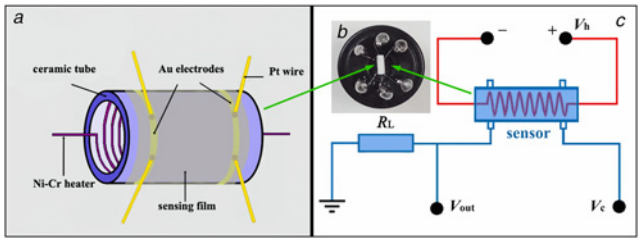

Fig. 1 *Sensor element and sensor measurement system*
a Schematic of an alumina ceramic tube as a sensor element
b Photograph of an alumina ceramic tube as a sensor element
c Schematic circuit of gas sensor measurement system

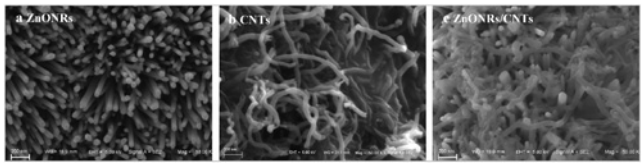

Fig. 2 *SEM images of*
a ZnONRs
b MWCNTs
c ZnONRs/MWCNTs nanocomposite

The TEM images of the ZnONRs/MWCNTs nanocomposite are shown in Fig. 3. Fig. 3*a* confirms the rod-like morphology of the ZnO and the tube morphology of the CNTs. Fig. 3*b* shows the HR-TEM image of the contact between a CNT and a ZnONR. The lattice fringe spacing of the ZnONR is about 0.26 nm, corresponding to the interplanar distance of the (002) crystal planes of the wurtzite ZnO, indicating that the ZnONR grows along the ⟨001⟩ crystallographic direction. The typical interlayer spacing of MWCNT is determined to be 0.35 nm.

Fig. 4 shows the XRD patterns of the ZnONRs, MWCNTs, and ZnONRs/MWCNTs nanocomposite. The diffraction peaks at 31.8°, 34.4°, 36.3°, 47.5°, 56.6°, 62.9°, 66.4°, 68.0° and 69.1° are corresponding to the (100), (002), (101), (102), (110), (103), (200), (112), and (201) planes of crystalline ZnO with a hexagonal wurtzite structure (JCPDS Card No. 36–1451). In Fig. 4*b*, the broad peak at ~26° is attributed to the graphitic (002) plane, known as the main peak of CNTs (JCPDS Card No. 41–1487)[16]. Two weak peaks at 42.7° and 44.3° are graphitic (100) and (101) planes from the CNTs. All the major peaks of ZnO and CNTs are observed in the XRD pattern of the ZnONRs/MWCNTs nanocomposite shown in Fig. 4*c*, meaning that the MWCNTs were successfully decorated on the ZnONRs.

The responses of the ZnONRs, MWCNTs, and ZnONRs/MWCNTs nanocomposite sensors to 100 ppm ethanol were first checked at different temperatures ranging from 240 to 400 °C to optimise the working temperature. As shown in Fig. 5, the temperature has an obvious influence on the responses of three sensors. When the temperature is 240°C, the response gap of the three sensors is small. With the increase of the temperature, the responses of all sensors first increase and then reach the maximum at 370°C. However, the response of the ZnONRs/MWCNTs nanocomposite sensor increases much more quickly than those of ZnONRs and MWCNTs sensors. At the optimal temperature of 370°C, the maximum response value for the ZnONRs/MWCNTs nanocomposite sensor is 26.1, which is more than two times higher than those of ZnONR (10.4) and MWCNTs (5.1) sensors. The responses of the three sensors begin to decrease after further increasing the working temperature to 400°C.

Fig. 6*a* depicts the dynamic response–recovery curves of the ZnONRs, MWCNTs, and ZnONRs/MWCNTs gas sensors when exposed to different ethanol concentrations at 370°C. The ZnONRs/MWCNTs sensor exhibits the highest sensitivity compared with the MWCNTs sensor and the ZnONRs sensor under various ethanol concentrations. The response gaps between the ZnONRs/MWCNTs sensors and the other two sensors are small at low concentration of ethanol. However, at high ethanol concentration, the gaps become much larger. For example, the responses of the ZnONRs and ZnONRs/MWCNTs sensors are close to each other (1.78 for the ZnONR sensor and 1.93 for the ZnONRs/MWCNTs sensor) to 2 ppm ethanol, while the response of the ZnONRs/MWCNTs sensor is more than two times higher than that of the ZnONRs sensor to 100 ppm ethanol. The enhanced response for the ZnONRs/MWCNTs sensor is due to the higher surface area of the ZnONRs/MWCNTs nanocomposite. The higher surface area is beneficial to the adsorption of more gas and therefore the gas concentration is larger to reach the saturation value of the response. As shown in the response versus ethanol concentration curve (Fig. 6*b*), the response of ZnONRs and MWCNTs sensors reach saturation at about 400 and 100 ppm,

doi: 10.1049/mnl.2017.0775

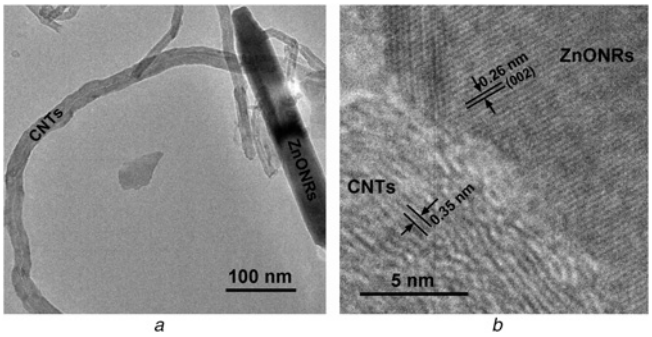

Fig. 3 *TEM images of ZnONRs/MWCNTs nanocomposite*

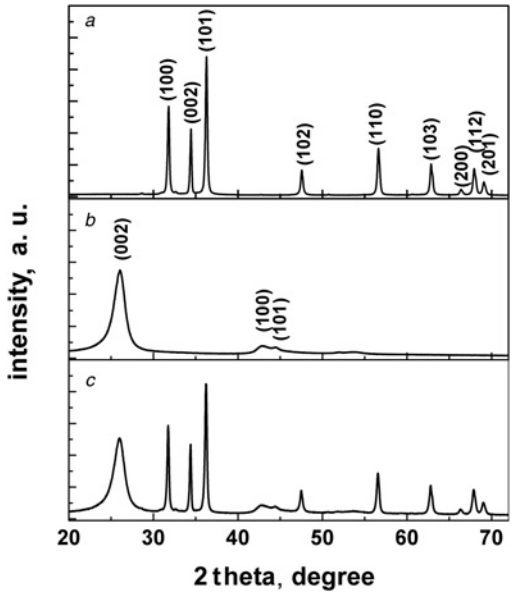

Fig. 4 *XRD patterns of*
a ZnONRs
b MWCNTs
c ZnONRs/MWCNTs nanocomposite

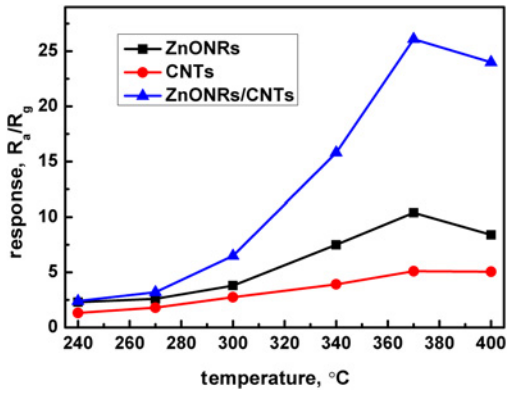

Fig. 5 *Responses of the ZnONRs sensor, MWCNTs sensor, and the ZnONRs/MWCNTs nanocomposite sensor to 100 ppm ethanol vapour at different working temperatures*

respectively. While the response of the ZnONRs/MWCNTs sensor reaches saturation at about 600 ppm. A linear relation between the response and the ethanol concentration is obtained when the concentration is below 20 ppm, as shown in the inset of Fig. 6*b*.

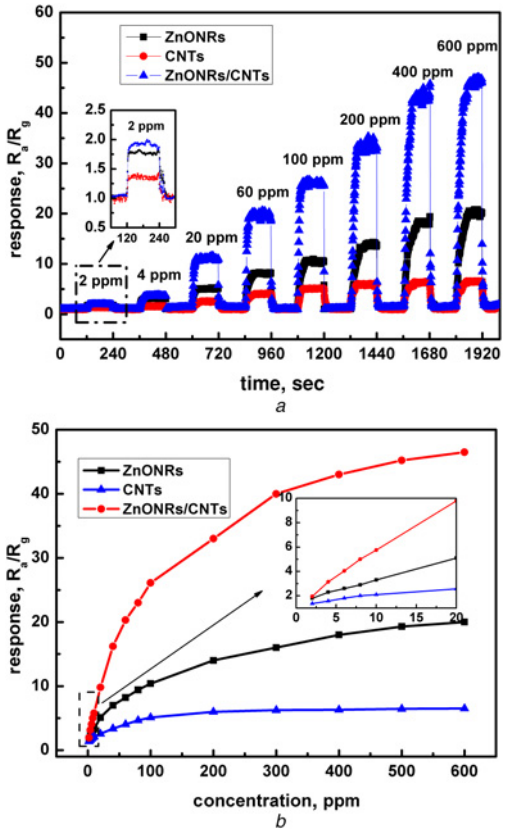

Fig. 6 *Response of the ZnONRs MWCNTs, and ZnONRs/MWCNTs nanocomposite sensors to ethanol in the concentration range of 2–600 ppm at 370 °C*
a Response versus time curves
b Response versus ethanol concentration curves

Fig. 7 shows the dynamic response–recovery curve of the ZnONRs, MWCNTs, and the ZnONRs/MWCNTs nanocomposite gas sensors to 100 ppm ethanol at 370°C. The response time and recovery time are 2 and 16 s, respectively, for the ZnONRs/MWCNTs gas sensor, which is much shorter than those of the ZnONRs sensor (9 and 20 s) and the MWCNTs sensor (12 and 24 s). Such a quick response of the ZnONRs/MWCNTs gas sensor makes it more suitable for real-time online detection of ethanol and can be attributed to the reduction of the resistance. As shown in Fig. 7, the original resistance of MWCNTs is three orders lower than those of ZnONRs and ZnONRs/MWCNTs, which confirms the well electric conductivity of the MWCNTs. Moreover, the resistance of ZnONRs/MWCNTs is much smaller than that of ZnONRs due to the high electron transport velocity of the MWCNTs.

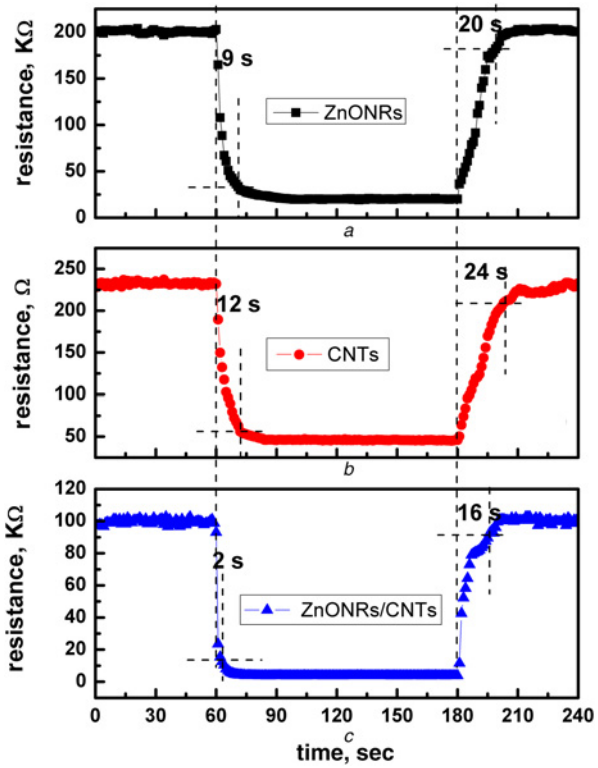

Fig. 7 *Response–recovery curves of the ZnONRs, MWCNTs, and ZnONRs/MWCNTs nanocomposite sensors to 100 ppm ethanol at 370°C*

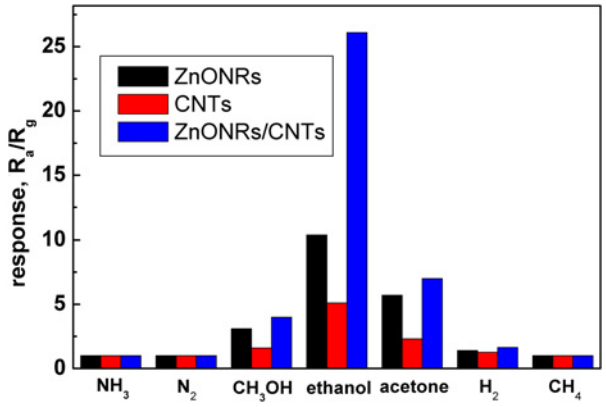

Fig. 8 *Responses of the ZnONRs sensor, MWCNTs sensor, and the ZnONRs/MWCNTs nanocomposite sensor to 100 ppm various gases at 370°C*

The selectivity is another key parameter for the evaluation of gas sensor. Ammonia (NH_3), nitrogen (N_2), methanol (CH_3OH), acetone (CH_3COCH_3), hydrogen (H_2), and methane (CH_4) were chosen to study the selectivity of the ZnONRs, MWCNTs, and ZnONRs/MWCNTs sensors. Fig. 8 depicts the responses of three sensors to different gases with a concentration of 100 ppm at 370°C. All of the sensors show a weak response towards NH_3, N_2, H_2, and CH_4. The responses of the ZnONRs sensor to acetone and methanol are 5.7 and 3.1, respectively, which are much lower than that (10.4) to ethanol. The responses of the ZnONRs/MWCNTs sensor to acetone and methanol are 7.0 and 4.0, respectively, which are also much lower than that (26.1) to ethanol. Although all of the three sensors exhibit selectivity to ethanol, the ZnONRs/MWCNTs sensor shows better selectivity compared with the ZnONRs sensor and the CNTs sensor. The better selectivity of the ZnONRs/MWCNTs sensor to ethanol may due to the different optimal temperatures of various gases

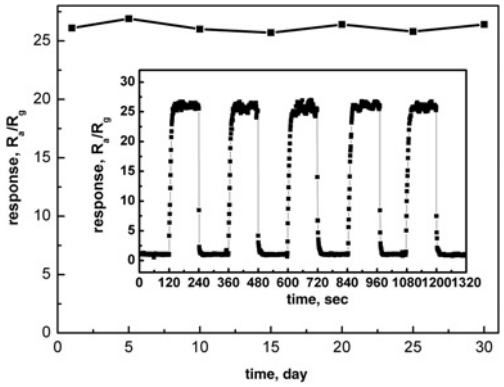

Fig. 9 *Stability and repeatability studies of the ZnONRs/MWCNTs nanocomposite sensor exposed to 100 ppm ethanol at 370°C*

and the specific morphology of the ZnONRs/MWCNTs nanocomposite [2, 20, 27].

Stability and repeatability are also two important performance indices and low stability is the main drawback of the sensors made with ZnO nanocrystals [28]. The long-term performances of the ZnONR/MWCNT sensors were studied by testing the response curves for 30 days, as shown in Fig. 9. A swing <3.1% of response is obtained for the sensor for 30 days. The inset of Fig. 9 shows five-continuous response-recovery cycles as the ZnONRs/MWCNTs sensor is alternately exposed to air and 100 ppm ethanol at 370°C. It can be seen that the ZnONRs/MWCNTs sensor maintains its initial response without an obvious attenuation and shift. The results indicate that the ZnONRs/MWCNTs sensor exhibits well stability and repeatability, which makes it more promising for practical application. A traditional gas sensor fabrication process often needs to collect the obtained nanostructures and coat them onto the measuring element surface. This process may change or destroy the initial characteristics of the nanostructures and induce the instability of the sensor. In this Letter, the ZnONRs were directly grown onto the measuring element surface, which is the possible reason for the long-term stability of the ZnONRs/MWCNTs sensor.

The sensing mechanism of ZnO nanostructures can be described by the adsorption–desorption processes on the surface of ZnO nanostructures [1, 29, 30]. When the ZnO nanostructures are exposed to air, their surfaces will absorb the surrounding oxygen molecules. The absorbed oxygen molecules capture electrons from the conduction band of ZnO and are ionised to O_2^-, O^-, and O^{2-}, resulting in the formation of an electron depletion layer on the ZnO surface and an increase of resistance. While when the ZnO nanostructures are exposed to the reductive gas, for example, ethanol, the surface oxygen ions will react with the gas and simultaneously electrons are donated back to ZnO, causing a decrease of resistance. Compared with ZnONRs, the ZnONRs/MWCNTs nanocomposite exhibits improved ethanol sensing performances, such as, high response, short response time and recovery time, which may ascribe to synergistic effects of the following reasons. (i) ZnONRs/MWCNTs possess a large specific surface area because of their tubular structures of MWCNTs, which can absorb more target gas and enhance the response of the sensor. (ii) The contact resistance of individual ZnONRs is generally large due to the limit of the electron transport between nanorods [30]. CNTs exhibit excellent electron transport capability and can serve as highly conductive channels between ZnONRs. Therefore, the adding of CNTs can enhance the electron transport velocity and reduce the response and recovery times.

4. Conclusion: MWCNTs were assembled on the surfaces of the ZnONRs grown directly on the alumina ceramic tube to form the

doi: 10.1049/mnl.2017.0775

ZnONR/MWCNT nanocomposite sensor. Better ethanol sensing performances were achieved for the ZnONR/MWCNT sensor in comparison with the ZnONR sensor and the CNT sensor, including higher response, shorter response and recovery times, better selectivity and stability. A response time as short as 2 s and a recovery time of 16 s are obtained for the ZnONR/MWCNT sensor. The excellent sensing performances of the ZnONR/MWCNT sensor are due to the synergistic effects of the ZnONRs and MWCNTs, including the large specific surface area and high electron transport capability. The Letter demonstrates that the ZnONR/MWCNT nanocomposite has potential application for the ethanol gas sensors, especially for real-time online ethanol sensors.

5. Acknowledgments: This work was supported by the National Natural Science Foundation of China (grant nos. 61504096 and 61401306), the National Key Research and Development Plan Project (grant no. 2016YFB0402703), the Natural Science Foundation of Tianjin (grant nos. 16JCYBJC16300, 15JCYBJC24000, and 17JCZDJC32600), the program for scientific and technological special commissioner of Tianjin (grant no. 16JCTPJC50800), and the Youth Top-notch Talents Program of Tianjin.

6 References

[1] Sun Y.-F., Liu S.-B., Meng F.-L., *ET AL.*: 'Metal oxide nanostructures and their gas sensing properties: a review', *Sensors*, 2012, **12**, pp. 2610–2631

[2] Du J., Zhao R., Chen S., *ET AL.*: 'Self-Assembly of gridlike zinc oxide lamellae for chemical-sensing applications', *ACS Appl. Mater. Interfaces*, 2015, **7**, pp. 5870–5878

[3] Kumar R., Al-Dossary O., Kumar G., *ET AL.*: 'Zinc oxide nanostructures for NO_2 gas-sensor applications: a review', *Nano-Micro Lett.*, 2015, **7**, pp. 97–120

[4] Wei S., Wang S., Zhang Y., *ET AL.*: 'Different morphologies of ZnO and their ethanol sensing property', *Sens. Actuators B, Chem.*, 2014, **192**, pp. 480–487

[5] Luo J., Ma S. Y., Sun A. M., *ET AL.*: 'Ethanol sensing enhancement by optimizing ZnO nanostructure: from 1D nanorods to 3D nanoflower', *Mater. Lett.*, 2014, **137**, pp. 17–20

[6] Tesfamichael T., Cetin C., Piloto C., *ET AL.*: 'The effect of pressure and W-doping on the properties of ZnO thin films for NO_2 gas sensing', *Appl. Surf. Sci.*, 2015, **357**, pp. 728–734

[7] Woo H.-S., Kwak C.-H., Chung J.-H., *ET AL.*: 'Highly selective and sensitive xylene sensors using Ni-doped branched ZnO nanowire networks', *Sens. Actuators B, Chem.*, 2015, **216**, pp. 358–366

[8] Zhang P., Pan G., Zhang B., *ET AL.*: 'High sensitivity ethanol gas sensor based on Sn-doped ZnO under visible light irradiation at low temperature', *Mater. Res.-Ibero-Am. J.*, 2014, **17**, pp. 817–822

[9] Wan G.X., Ma S.Y., Li X.B., *ET AL.*: 'Synthesis and acetone sensing properties of Ce-doped ZnO nanofibers', *Mater. Lett.*, 2014, **114**, pp. 103–106

[10] Li W., Ma S., Yang G., *ET AL.*: 'Preparation, characterization and gas sensing properties of pure and Ce doped ZnO hollow nanofibers', *Mater. Lett.*, 2015, **138**, pp. 188–191

[11] Naghadeh S.B., Vahdatifar S., Mortazavi Y., *ET AL.*: 'Functionalized MWCNTs effects on dramatic enhancement of MWCNTs/SnO_2 nanocomposite gas sensing properties at low temperatures', *Sens. Actuators B, Chem.*, 2016, **223**, pp. 252–260

[12] Aroutiounian V.M., Adamyan A.Z., Khachaturyan E.A., *ET AL.*: 'Study of the surface-ruthenated SnO_2/MWCNTs nanocomposite thick-film gas sensors', *Sens. Actuators B, Chem.*, 2013, **177**, pp. 308–315

[13] Ahmadnia-Feyzabad S., Khodadadi A.A., Vesali-Naseh M., *ET AL.*: 'Highly sensitive and selective sensors to volatile organic compounds using MWCNTs/SnO_2', *Sens. Actuators B Chem.*, 2012, **166**, pp. 150–155

[14] Afzali P., Abdi Y., Arzi E.: 'Directional reduction of graphene oxide sheets using photocatalytic activity of ZnO nanowires for the fabrication of a high sensitive oxygen sensor', *Sens. Actuators B, Chem.*, 2014, **195**, pp. 92–97

[15] Chen P.C., Sukcharoenchoke S., Ryu K., *ET AL.*: '2,4,6-Trinitrotoluene (TNT) chemical sensing based on aligned single-walled carbon nanotubes and ZnO nanowires', *Adv. Mater.*, 2010, **22**, p. 1900– +

[16] Farbod M., Joula M.H., Vaezi M.: 'Promoting effect of adding carbon nanotubes on sensing characteristics of ZnO hollow sphere-based gas sensors to detect volatile organic compounds', *Mater. Chem. Phys.*, 2016, **176**, pp. 12–23

[17] Oweis R.J., Albiss B.A., Al-Widyan M.I., *ET AL.*: 'Hybrid zinc oxide nanorods/carbon nanotubes composite for nitrogen dioxide gas sensing', *J. Electron. Mater.*, 2014, **43**, pp. 3222–3228

[18] Varghese O.K., Kichambre P.D., Gong D., *ET AL.*: 'Gas sensing characteristics of multi-wall carbon nanotubes', *Sens. Actuators B, Chem.*, 2001, **81**, pp. 32–41

[19] Kauffman D.R., Star A.: 'Carbon nanotube Gas and vapor sensors', *Angew. Chem. Int. Ed.*, 2008, **47**, pp. 6550–6570

[20] Shan H., Liu C.B., Liu L., *ET AL.*: 'Excellent ethanol sensor based on multiwalled carbon nanotube-doped ZnO', *Chinese Sci. Bull.*, 2014, **59**, pp. 374–378

[21] Khanderi J., Hoffmann R.C., Gurlo A., *ET AL.*: 'Synthesis and sensoric response of ZnO decorated carbon nanotubes', *J. Mater. Chem.*, 2009, **19**, pp. 5039–5046

[22] Hernandez S.C., Hangarter C.M., Mulchandani A., *ET AL.*: 'Selective recognition of xylene isomers using ZnO-SWNTs hybrid gas sensors', *Analyst*, 2012, **137**, pp. 2549–2552

[23] Hernandez S.C., Kakoullis J., Lim J.H., *ET AL.*: 'Hybrid ZnO/SWNT nanostructures based gas sensor', *Electroanalysis*, 2012, **24**, pp. 1613–1620

[24] Ju D., Xu H., Zhang J., *ET AL.*: 'Direct hydrothermal growth of ZnO nanosheets on electrode for ethanol sensing', *Sens. Actuators B, Chem.*, 2014, **201**, pp. 444–451

[25] Wang P., Wang D., Zhang M., *ET AL.*: 'ZnO nanosheets/graphene oxide nanocomposites for highly effective acetone vapor detection', *Sens. Actuators B, Chem.*, 2016, **230**, pp. 477–484

[26] Van Hieu N., Duc N.A.P., Trung T., *ET AL.*: 'Gas-sensing properties of tin oxide doped with metal oxides and carbon nanotubes: a competitive sensor for ethanol and liquid petroleum gas', *Sens. Actuators B, Chem.*, 2010, **144**, pp. 450–456

[27] Wang J.X., Sun X.W., Yang Y., *ET AL.*: 'Hydrothermally grown oriented ZnO nanorod arrays for gas sensing applications', *Nanotechnology*, 2006, **17**, pp. 4995–4998

[28] Xiao Y., Lu L., Zhang A., *ET AL.*: 'Highly enhanced acetone sensing performances of porous and single crystalline ZnO nanosheets: high percentage of exposed (100) facets working together with surface modification with Pd nanoparticles', *ACS Appl. Mater. Interfaces*, 2012, **4**, pp. 3797–3804

[29] Miller D.R., Akbar S.A., Morris P.A.: 'Nanoscale metal oxide-based heterojunctions for gas sensing: A review', *Sens. Actuators B, Chem.*, 2014, **204**, pp. 250–272

[30] Alenezi M.R., Henley S.J., Emerson N.G., *ET AL.*: 'From 1D and 2D ZnO nanostructures to 3D hierarchical structures with enhanced gas sensing properties', *Nanoscale*, 2014, **6**, pp. 235–247